

Dynamics of cell-type transition mediated by epigenetic modifications

Rongsheng Huang^a, Qiaojun Situ^b, Jinzhi Lei^{c,*}

^a*School of Science, Jimei University, Xiamen Fujian 361021, China*

^b*Zhou Pei-Yuan Center for Applied Mathematics, Tsinghua University, Beijing 100084, China*

^c*School of Mathematical Sciences, Center for Applied Mathematics, Tiangong University, Tianjin, 300387, China*

Abstract

Maintaining tissue homeostasis requires appropriate regulation of stem cell differentiation. The Waddington landscape posits that gene circuits in a cell form a potential landscape of different cell types, wherein cells follow attractors of the probability landscape to develop into distinct cell types. However, how adult stem cells achieve a delicate balance between self-renewal and differentiation remains unclear. We propose that random inheritance of epigenetic states plays a pivotal role in stem cell differentiation and present a hybrid model of stem cell differentiation induced by epigenetic modifications. Our comprehensive model integrates gene regulation networks, epigenetic state inheritance, and cell regeneration, encompassing multi-scale dynamics ranging from transcription regulation to cell population. Through model simulations, we demonstrate that random inheritance of epigenetic states during cell divisions can spontaneously induce cell differentiation, dedifferentiation, and transdifferentiation. Furthermore, we investigate the influences of interfering with epigenetic modifications and introducing additional transcription factors on the probabilities of dedifferentiation and transdifferentiation, revealing the underlying mechanism of cell reprogramming. This *in silico* model provides valuable insights into the intricate mechanism governing stem cell differentiation and cell reprogramming and offers a promising path to enhance the field of regenerative medicine.

Keywords: stem cell differentiation; epigenetic state; Waddington landscape; cell reprogramming; multi-scale model

1. Introduction

Adult stem cells play a vital role in maintaining tissue homeostasis by replenishing dying cells and regenerating damaged tissues through controlled self-renewal and differentiation[1]. Understanding the mechanism underlying cell

*Corresponding author: jzlei@tiangong.edu.cn

fate decisions and the regulation of self-renewal and differentiation in stem cell biology is of utmost significance.

Waddington's epigenetic landscape is a fundamental concept in comprehending cell fate decisions and cell differentiation[2]. The landscape analogy visualizes a cell as a ball rolling on a mountain, with valleys representing stable cell phenotype and ridges signifying cell fate choice leading to new phenotypes. While Waddington's epigenetic landscape provides an intuitive understanding of the biological process, the mechanisms driving cellular development and reprogramming remain elusive[3]. Specifically, how gene circuits define Waddington's epigenetic landscape in a multicellular system, the driving force behind cell fate decision, and how adult stem cell systems balance self-renewal and differentiation pose intriguing questions.

Gene circuits consisting of two transcription factors, such as PU.1-GATA1 or SOX2-OCT4, have been extensively studied as they are associated with cell fate decisions[4, 5, 6, 7]. These circuits exhibit three stable equilibrium points corresponding to stem cells and two differentiated cell fates, validating the concepts of Waddington landscape. The regulatory interplay between these transcription factors determines cell fate. Despite such discoveries, the driving force triggering cell-type switches remains a topic of debate, with stochastic fluctuation, gene regulation, cell-cell communications, and artificial induction being proposed as potential mechanisms[8, 9, 10, 11, 12, 13, 14, 15, 16]. Remarkably, self-renewal and differentiation of stem cells maintain a state of dynamic equilibrium even in the face of random environmental changes. This highlights the importance of regulating the transitions between cell types during stem cell regeneration to ensure reliable tissue function.

Recent advancements in single-cell sequencing techniques have illuminated cell heterogeneity, revealing macro-heterogeneities in gene expression among cells with different phenotypes and even microscopic heterogeneity within cells of the same phenotype[17, 18, 19, 20, 21, 22, 23]. Epigenetic regulation, encompassing histone modification and DNA methylation, has emerged as a key player in cellular heterogeneity and phenotype switching[24, 25, 26, 27].

Histones are structural chromosome proteins, including H1 and H3, H4, H2A, and H2B subunits. There are various forms and multiple functions of histone modifications that regulate gene expression. For instance, trimethylation of lysine 4 on histone H3 protein subunit (H3K4me3) and H4K12 acetylation can promote gene expression, while ubiquitination, such as ub-H2A, can inhibit gene expression[28, 29]. Histone modifications are heritable during cell division. The parental modifications are recognized by a binding protein or a reading protein, which then recruits a chromatin modifier or writer protein to alter the histone modifications[30].

DNA methylation is a process where methyl(CH₃) group is added to DNA, which can alter the function of genes and impact gene expression. Both histone modifications and DNA methylation inheritance are semi-conservative but inevitably accompanied by natural changes during each generation, which may lead to cell heterogeneity and plasticity[31].

In this study, we present a hybrid model of stem cell regeneration that in-

incorporates cell phenotype changes induced by epigenetic modifications. The model integrates a gene regulation network, epigenetic state inheritance, and cell regeneration, enabling multi-scale dynamics from transcription regulation to cell population. Through model simulations, we explore how random inheritance of epigenetic states during cell division can automatically induce cell differentiation, dedifferentiation, and transdifferentiation. Our *in silico* model offers valuable insights into the mechanism of stem cell differentiation and cell reprogramming.

2. Hybrid model of stem cell differentiation

The hybrid model established in this study is illustrated in Figure 1. It consists of individual-based modeling of a multi-cellular system (Fig. 1A), a gene regulation network (GRN) dynamics of two genes that self-activate and repress each other (Fig. 1B), a G0 cell cycle model for cell regeneration (Fig. 1C), and stochastic inheritance of epigenetic states during cell divisions (Fig. 1D). The three types of dynamics are coupled with each other through the cell cycle processes and cell-type transitions. The detailed formulations of the model are given below.

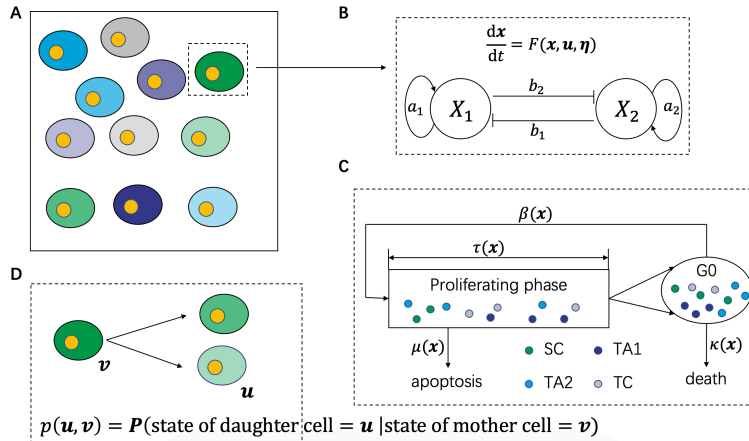


Figure 1: Illustration of the hybrid model. (A) Individual-based model of a multi-cellular system. (B) Dynamic system of gene circuit motif. (C) G0 cell cycle model of cell regeneration. (D) Stochastic inheritance of epigenetic state during cell divisions.

2.1. Gene regulation network

To investigate how epigenetic modifications can drive cell lineage commitment, we consider a GRN consisting of two master transcription factors (TFs)

X_1 and X_2 , which self-activate and repress each other (Fig. 1B). This gene network frequently appears in many cell-fate decision-making systems and has been extensively studied[7, 32, 33, 34, 35, 36, 37]. Mathematically, the gene network can be modeled using two different approaches: additive and multiplicative regulations, where the production rates from positive and negative feedbacks are either added or multiplied, respectively[4, 9]. This study adopts the additive modeling approach, following the model described in [9]. However, it is essential to note that the model formulations and results presented in this study are also consistent with multiplicative feedback regulations.

Let x_1 and x_2 represent the expression level (protein concentration) of genes X_1 and X_2 , respectively. The gene expression dynamics within one cell cycle are modeled with the following ordinary differential equations:

$$\begin{cases} \frac{dx_1}{dt} = a_1 \left(\rho_1 + (1 - \rho_1) \frac{x_1^n}{s_1^n + x_1^n} \right) + b_1 \frac{s_2^n}{s_2^n + x_2^n} - k_1 x_1, \\ \frac{dx_2}{dt} = a_2 \left(\rho_2 + (1 - \rho_2) \frac{x_2^n}{s_2^n + x_2^n} \right) + b_2 \frac{s_1^n}{s_1^n + x_1^n} - k_2 x_2, \end{cases} \quad (1)$$

where $a_1, a_2, \rho_1, \rho_2, s_1, s_2, n, b_1, b_2, k_1$, and k_2 are non-negative parameters. The parameters a_1 and a_2 denote the maximum expression rates of the self-activation of the two genes, while ρ_1 and ρ_2 ($0 \leq \rho_i \leq 1$) represent the ratios between the basal level to the maximum level of the regulation of each gene. The parameters b_1 and b_2 denote the basal expression rates of the two genes without repression. The parameters s_1 and s_2 represent the half-effective concentration of the two proteins X_1 and X_2 , respectively, in the transcription regulation, and n represents the corresponding Hill coefficient. The degradation rates of the two proteins are represented by k_1 and k_2 , respectively.

To address the influence of extrinsic noise perturbation, we introduced stochastic fluctuations to a_1 and a_2 , resulting in the following expressions:

$$a_i(\eta_i) = \alpha_i e^{\sigma_i \eta_i - \sigma_i^2 / 2}, \quad i = 1, 2,$$

where α_1 and α_2 are positive parameters to represent the average expression rates. Here, σ_1 and σ_2 represent the intensities of the noise perturbations, and η_1 and η_2 are color noises defined by the Ornstein-Uhlenbeck processes:

$$d\eta_i = -(\eta_i / \zeta_i) dt + \sqrt{2 / \zeta_i} dW_i(t), \quad i = 1, 2, \quad (2)$$

where $W_1(t)$ and $W_2(t)$ are independent Wiener process, and ζ_1 and ζ_2 are relaxation coefficients. In the stationary state, we have $E(a_i(\eta_i)) = \alpha_i$ and $E(\eta_i(t_1)\eta_i(t_2)) = e^{-|t_1 - t_2| / \zeta_i}$ ($i = 1, 2$), where $E(\cdot)$ represents the mathematical expectation.

To further account for the effects of epigenetic modification on gene regulation dynamics, it is known that epigenetic regulations, such as histone modification or DNA methylation, can interfere with chromatin structure and alter the basal expression rates. Therefore, we introduced the assumption that the expression levels a_1 and a_2 are dependent on the epigenetic modification state

of the two genes, denoted by u_1 and u_2 , respectively. Here, by the epigenetic state, we mean the fractions of marked nucleosomes or methylated CpG sites in a DNA segment of interest. Hence, the epigenetic state $\mathbf{u} = (u_1, u_2)$ is assumed to lie in the domain $\Omega = [0, 1] \times [0, 1]$. Additionally, we considered that the epigenetic states u_1 and u_2 undergo random changes only during cell division, which is discussed in more detail below.

Since epigenetic states primarily affect chromatin structure, they might influence the chemical potential required to initiate the transcription process. Thus, along with the extrinsic noise perturbations, we can express the expression rates a_1 and a_2 as follows

$$a_i(u_i, \eta_i) = \alpha_i e^{\lambda_i u_i} e^{\sigma_i \eta_i - \sigma_i^2/2}, \quad i = 1, 2, \quad (3)$$

where $\lambda_i (i = 1, 2)$ represent the impact of the epigenetic modification states on the expression levels. Specifically, $\lambda_i > 0$ indicates an epigenetic modification that enhances the strength of self-activation, while $\lambda_i < 0$ indicates a modification that reduces this strength.

The expression state $\mathbf{x} = (x_1, x_2)$ depends on the epigenetic state $\mathbf{u} = (u_1, u_2)$ within one cell cycle through equations (1)-(3). With properly selected parameter values, the model exhibits three stable steady states that correspond to three cell types (see Fig. 2 below). For instance, the PU.1-GATA1 motif is involved in the gene circuit that determines the cell fate of erythroid/megakaryocyte lineages from granulocyte/monocyte lineages. PU.1 and GATA1 are expressed in the precursor cells (PC). Specifically, the granulocyte/monocyte lineage (GMC) cells exhibit low PU.1 expression and high GATA1 expression, while erythroid/megakaryocyte lineage (EMC) cells show high GATA1 expression and low PU.1 expression. For the sake of generality, we refer to the three cell types as stem cell (SC), transit-amplifying cell 1 (TA1), and transit-amplifying cell 2 (TA2). Additionally, we use transition cells (TC) for cells not classified as SC, TA1, or TA2. Mathematically, the phenotypes are defined from $\mathbf{x} = (x_1, x_2)$ as (see Section 3.1 below):

$$\text{phenotype} = \begin{cases} \text{SC} : & \text{both } X_1 \text{ and } X_2 \text{ are medium expression,} \\ \text{TA1} : & X_1 \text{ is high expression and } X_2 \text{ is low expression,} \\ \text{TA2} : & X_1 \text{ is low expression and } X_2 \text{ is high expression,} \\ \text{TC} : & \text{otherwise.} \end{cases} \quad (4)$$

We note that both positive and negative feedback parameters a_i and b_i are subjected to noise perturbation and epigenetic regulations. Here, we only consider the changes in the positive feedback parameters for the simplicity of model introduction and discussions. The methods and results in this study can be extended to general cases with modifications in both feedback parameters.

Our model formulates random perturbations to expression rate by multiplying the log-normal distribution random number defined by an Ornstein-Uhlenbeck process. This type of formulation was introduced in our previous studies[38] and differs from the conventional Langevin approach. Biologically,

gene expression rates have been observed to follow a log-normal distribution rather than a normal distribution[39]. Mathematically, using the expression in equation (3) can prevent the possible negative expression rate, which can be problematic when adding a Gaussian perturbation to the expression rate a_i . This formulation is biologically more appropriate for modeling extrinsic random perturbations.

2.2. G0 cell cycle model

To incorporate the above gene regulation network dynamics with cell division, we referred to the G0 cell cycle model of heterogeneous cell regeneration [40, 41, 42]. In this model, we only consider cells with the ability to undergo cell cycling, and each cell has different rates of proliferation and cell death dependent on its cell phenotypic (SC, TA1, TA2, or TC). Cells that have lost the ability to undergo cell cycling were not considered and were removed from the system. The cycling cells are classified into resting (G0) or proliferating phases. Resting phase cells can either re-enter the proliferating phase with a rate β or be removed from the resting phase with a rate κ due to cell death or senescence. Proliferating phase cells can either randomly exit with a rate μ due to apoptosis or divide into two daughter cells after a time τ following entry into the proliferative compartment (Fig. 1C). The kinetic rates of each cell, including the proliferation rate β , the removal rate κ , the apoptosis rate μ , and the proliferation duration τ depend on the corresponding cell phenotype.

The SC, TA1, TA2, and TC cells differ in their regulation of cell proliferation. For SCs, the self-renewal ability is biologically associated with microenvironmental conditions and intracellular signaling pathways [43, 44]. Despite the complexity of signaling pathways, the phenomenological formulation of the Hill function dependence can be derived from simple assumptions regarding the interactions between signaling molecules and receptors [41, 45], and is given by

$$\beta_{\text{SC}} = \beta_0 \frac{\theta}{\theta + Q(t)},$$

where $Q(t)$ represents the number of SC at time t , β_0 represents the maximum proliferation rate, and θ is a constant for the half-effective cell number. We define the removal rate κ , the apoptosis rate μ , and the proliferation duration τ of stem cells as:

$$\kappa_{\text{SC}} = \kappa_0, \quad \mu_{\text{SC}} = \mu_0, \quad \tau_{\text{SC}} = \tau_0.$$

For TA1 or TA2 cells, we assumed that they have unconstrained proliferation rates, higher removal rates, and shortened proliferation durations than stem cells. Moreover, each TA1 or TA2 cell has a limited ability of cell divisions, *i.e.*, a TA1 or TA2 cell will be removed from the system when it reaches the maximum cell division times (here we set it as 15). Hence, we have

$$\begin{aligned} \beta_{\text{TA1}} = \beta_{\text{TA2}} = \beta_0, \quad \mu_{\text{TA1}} = \mu_{\text{TA2}} = \mu_0, \quad \tau_{\text{TA1}} = \tau_{\text{TA2}} = \tau_0/2, \\ \kappa_{\text{TA1}} = \kappa_{\text{TA2}} = \begin{cases} 2\kappa_0, & \text{divisions} < 15, \\ +\infty, & \text{divisions} \geq 15, \end{cases} \end{aligned}$$

The transition state is usually very short between cell divisions; hence, cell proliferation and apoptosis are not considered for TCs. Thus, we set

$$\beta_{\text{TC}} = \mu_{\text{TC}} = \tau_{\text{TC}} = \kappa_{\text{TC}} = 0.$$

Table 1 summarizes the kinetic rates for different phenotypes.

Table 1: The kinetic rates for different phenotype

cell phenotype	β	κ	μ	τ
SC	$\beta_0\theta/(\theta + Q)$	κ_0	μ_0	τ_0
TA1	β_0	$2\kappa_0$ or $+\infty$	μ_0	$\tau_0/2$
TA2	β_0	$2\kappa_0$ or $+\infty$	μ_0	$\tau_0/2$
TC	0	0	0	0

From the above model description, given the epigenetic state $\mathbf{u} = (u_1, u_2)$ of each cell, the gene expression state $\mathbf{x} = (x_1, x_2)$ dynamically evolves according to the stochastic differential equations (1)-(3). Accordingly, the cell phenotype and the kinetic rates β , κ , μ and τ can change during a cell cycle. In stochastic simulations, we model each cell's random proliferation, apoptosis, and cell-type switches in a multiple-cell system. Each cell has its cell state and randomly undergoes proliferation, apoptosis, and death with a probability depending on the cell state. Finally, when a cell undergoes mitosis, the cell divides into two cells, and the epigenetic states of the two daughter cells are calculated based on the inheritance probability functions below.

The effect of cell volume change was not considered in the model. Cell growth and volume changes are important biological processes and play important roles in cell-fate decisions[46, 47]. Moreover, biological mechanisms controlling cell growth and division are complicated and unclear for mammalian cells[48, 49, 50]. In this study, to avoid the complexity and be more focused on the epigenetic regulations, we assumed that the volume is unchanged during cell cycling so that cell growth does not affect the protein concentration.

2.3. Stochastic inheritance of epigenetic states

Histone modifications and DNA methylations in the daughter cells are reconstructed during cell division based on those in the mother cells. The epigenetic states of the daughter cells usually differ from those of their mother cells, and there is a random transition of the epigenetic states during cell division[30]. Moreover, the molecules (proteins and mRNAs) in the mother cells undergo random partition during mitosis, leading to their reallocation to the two daughter cells. Therefore, after mitosis, the epigenetic state \mathbf{u} and the expression level (protein concentration) \mathbf{x} of the model (1)-(3) for each newborn cell are reset. Here, for simplicity, we assumed symmetry division, meaning that the gene expression state \mathbf{x} of the two daughter cells is the same as that of the mother cell. However, the epigenetic state \mathbf{u} may undergo random transitions during cell division.

To model the stochastic inheritance of epigenetic states during cell division, we assumed that the epigenetic states of the two daughter cells are independent of each other, and we introduced an inheritance function $p(\mathbf{u}, \mathbf{v})$ to represent the conditional probability that a daughter cell of state \mathbf{u} comes from a mother cell of state \mathbf{v} after cell division. In other words,

$$p(\mathbf{u}, \mathbf{v}) = P(\text{state of daughter cell} = \mathbf{u} \mid \text{state of mother cell} = \mathbf{v}).$$

The inheritance function represents cell plasticity in each cell cycle, while the detailed biochemical processes of cell division are ignored. It is obvious to have

$$\int_{\Omega} p(\mathbf{u}, \mathbf{v}) d\mathbf{u} = 1, \quad \forall \mathbf{v} \in \Omega.$$

Biologically, the exact formulation of the inheritance function $p(\mathbf{u}, \mathbf{v})$ is difficult to determine, as it depends on the complex biochemical reactions during the cell division process. Nevertheless, while we consider $p(\mathbf{u}, \mathbf{v})$ as a conditional probability density, we focus on the epigenetic state before and after cell division and omit the intermediate complex process. This allows us to introduce a phenomenological function through numerical simulation based on a computational model of histone modification inheritance[41, 51, 52].

The states u_1 and u_2 represent the epigenetic states at two DNA segments corresponding to the gene X_1 and X_2 , respectively, and we assumed that they vary independently during cell division. If otherwise, we need further assumptions about their interdependence. Thus, we have

$$p(\mathbf{u}, \mathbf{v}) = p_1(u_1, \mathbf{v})p_2(u_2, \mathbf{v}), \quad (5)$$

where $p_i(u_i, \mathbf{v})$ represents the transition function of u_i , given the state \mathbf{v} of the mother cell. According to [51, 52], the normalized nucleosome modification level of daughter cells can be described by a random beta-distribution number dependent on the mother cell. Thus, we can write the inheritance function $p_i(u_i, \mathbf{v})$ through the density function of beta-distribution as

$$p_i(u_i, \mathbf{v}) = \frac{u_i^{g_i(\mathbf{v})-1} (1 - u_i)^{h_i(\mathbf{v})-1}}{B(g_i(\mathbf{v}), h_i(\mathbf{v}))}, \quad B(g, h) = \frac{\Gamma(g)\Gamma(h)}{\Gamma(g+h)}, \quad (6)$$

where $\Gamma(z)$ is the gamma function, $g_i(\mathbf{v})$ and $h_i(\mathbf{v})$ are shape parameters that depend on the epigenetic state of the mother cell. We assumed that the conditional expectation and conditional variance of u_i are (given the state \mathbf{v})

$$E(u_i|\mathbf{v}) = \phi_i(\mathbf{v}), \quad \text{Var}(u_i|\mathbf{v}) = \frac{1}{1 + \psi_i(\mathbf{v})} \phi_i(\mathbf{v})(1 - \phi_i(\mathbf{v})),$$

where the shape parameters can be expressed as

$$g_i(\mathbf{v}) = \psi_i(\mathbf{v})\phi_i(\mathbf{v}), \quad h_i(\mathbf{v}) = \psi_i(\mathbf{v})(1 - \phi_i(\mathbf{v})).$$

Here, we note that $\phi_i(\mathbf{v})$ and $\psi_i(\mathbf{v})$ always satisfy

$$0 < \phi_i(\mathbf{v}) < 1, \quad \psi_i(\mathbf{v}) > 0.$$

Hence, the inheritance function $p(\mathbf{u}, \mathbf{v})$ can be determined by the predefined conditional expectation and conditional variance, *i.e.*, the functions $\phi_i(\mathbf{u})$ and $\psi_i(\mathbf{u})$. Here, we assumed that $\psi_i(\mathbf{v})$ remains constant, while $\phi_i(\mathbf{v})$ increases with v_i and is expressed by a Hill function as:

$$\psi_i(\mathbf{v}) = m_0, \quad \phi_i(\mathbf{v}) = m_1 + m_2 \frac{(m_3 v_i)^{m_4}}{1 + (m_3 v_i)^{m_4}}, \quad \mathbf{v} = (v_1, v_2), \quad i = 1, 2, \quad (7)$$

where $m_j (j = 0, 1, 2, 3, 4)$ are all positive parameters.

From the above formulation, given the functions $\psi_i(\mathbf{v})$ and $\phi_i(\mathbf{v})$, the inheritance function $p(\mathbf{u}, \mathbf{v})$ can be expressed as a density function of beta-distribution random numbers.

2.4. Numerical scheme

The proposed hybrid model describes the dynamics of gene regulation networks and cell-type switches of individual cells in a multicellular system. Here, we present an individual-based numerical scheme aimed at simulating the dynamics of each cell in the system.

- **Initialization:** Set the time $t = 0$, the cell number N , and the state of all cells $\Sigma = \{[C_i(\mathbf{x}_i, \mathbf{u}_i)]_{i=1}^N\}$. Determine the phenotype (SC, TA1, TA2, or TC) and proliferation state (resting or proliferating phase) of each cell, and compute the count Q of stem cells. All cells are initially set as stem cells in the resting phase. Accordingly, set the division number of each cell as $\text{div}_i = 0$, and the corresponding age at the proliferating phase (starting from the entry of proliferating phase) as $a_i = 0$.
- **Iteration:** for t from 0 to T with a time step of Δt , do:
 - for each cell in Σ , do:
 - * Numerically solve equations (1)-(3) for a step Δt and update the expression state \mathbf{x} . If the cell is in the resting phase, update the phenotype of the cell based on the state \mathbf{x} .
 - * Calculate the proliferation rate β , the apoptosis rate μ , the terminate differentiation rate κ , and the proliferation duration τ .
 - * Determine the cell fate during the time interval $(t, t + \Delta t)$:
 - When the cell is at the resting phase, remove the cell from the simulating pool with a probability $\kappa \Delta t$, or enter the proliferating phase with a probability $\beta \Delta t$. If the cell enters the proliferating phase, set the age $a_i = 0$, and if the cell is a TA cell, set $\text{div}_i = \text{div}_i + 1$.

- When the cell is in the proliferating phase, if the age $a_i < \tau$, the cell is either removed (through apoptosis) with a probability $\mu\Delta t$, or remains unchanged and $a_i = a_i + \Delta t$. If the age $a_i \geq \tau$, the cell undergoes mitosis and divides into two cells. When mitosis occurs, set the state of two daughter cells following the rules below: set the age $a_i = 0$; set the epigenetic state \mathbf{u} of each daughter cell according to the inheritance probability function $p(\mathbf{u}, \mathbf{v})$; set the gene expression state \mathbf{x} as that of the mother cell.
- After mitosis, check the division number of TA cells. If the division number div_i of a TA cell is larger than the maximum value, remove the cell from the simulating pool.

end for

Update the system Σ with the cell number, epigenetic and gene expression states of all surviving cells, and the ages of the proliferating phase cells, and set $t = t + \Delta t$.

end for

In model simulations, we set the time step $\Delta t = 0.25\text{h}$. The numerical scheme can be implemented by the object-oriented programming language C++¹.

Table 2 lists the parameter values used in the current study. Here, the parameters illustrate the general process of phenotype switches due to epigenetic modifications along the cell regeneration process and are not specific to a particular type of cells. The parameters for the gene regulatory network were selected so that the corresponding gene network has multiple stable states for different cell types. The parameters for the epigenetic regulation were chosen so that cell-type transition can occur with a reasonable frequency. The parameter for cell regeneration (rate of proliferation, differentiation, and cell death) were taken per the biological restriction for the kinetic rates. Additionally, we only considered symmetric parameters, which means that $b_1 = b_2, k_1 = k_2, s_1 = s_2, \rho_1 = \rho_2, \alpha_1 = \alpha_2$. Nevertheless, the main results are insensitive to these parameter values.

3. Results

3.1. Phenotype defined by the epigenetic state of cells

To quantitatively define the phenotypes of SC and TA cells based on the gene expression state $\mathbf{x} = (x_1, x_2)$, we performed bifurcation analysis for the ordinary differential equation (1). Here, we assumed a symmetric situation so that $a_1 = a_2 = a$ and consider the bifurcation concerning the expression rate a . Figure 2A shows the dependence of the equilibrium state on the parameter a . When a is large ($a > 1.65$), there is a stable state steady with high expressions in both

¹The source codes are available at <https://github.com/jinzhilei/Cell-type-transition>.

Table 2: Parameter values for model simulation

Parameter	Description	Value	Unit ^(a)
b_1, b_2	Strengths of the mutual inhibition	1	AU \times h ⁻¹
k_1, k_2	Degradation rates of the proteins	1	AU \times h ⁻¹
s_1, s_2	50% effective concentration of the feedback loops	0.5	AU
ρ_1, ρ_2	The ratio between the basal level to the maximum level of the regulation of each gene	0.1	-
σ_1, σ_2	Intensity of the noise	0.05	-
ζ_1, ζ_2	Relaxation coefficient of the Ornstein-Uhlenbeck process	1	h ⁻¹
α_1, α_2	Expression rate of each gene	0.4	AU \times h ⁻¹
λ_1, λ_2	Impact coefficient of epigenetic modifications	1.9	-
n	Hill coefficient	4	-
m_0	constant	60	-
m_1	constant	0.08	-
m_2	constant	1.0	-
m_3	constant	2.0	-
m_4	Hill coefficient	2.0	-
θ	Constant for the half-effective cell number for SC population control	200	cells
β_0	Maximum proliferation rate	0.04	h ⁻¹
κ_0	The rate of removing cells out of the resting phase	0.01	h ⁻¹
μ_0	The apoptosis rate of cells in the proliferating phase	0.0002	h ⁻¹
τ_0	Proliferating phase time	4	h

^(a) AU means arbitrary unit.

X_1 and X_2 , which is denoted as $(+, +)$. When a decreases ($0.75 < a < 1.65$), in addition to the state $(+, +)$, there are two other stable steady states, one state has high expression in X_1 and low expression in X_2 ; the other one is opposite, with low expression in X_1 and high expression in X_2 . We denote these two states as $(+, +, -)$ and $(-, +, +)$, respectively. When a further decreases ($a < 0.75$), the state $(+, +)$ vanishes, and the two states $(+, +, -)$ and $(-, +, +)$ persist. Biologically, when a decreases from a large ($a > 1.65$) to a small ($a < 0.75$) value, the cell type $(+, +)$ emerge firstly, followed by the coexistence of the three states, and finally, transit to the cell type of either $(+, +, -)$ or $(-, +, +)$. This is akin to the differentiation of precursor cells to either granulocyte/monocyte lineage or erythroid/megakaryocyte lineage described with the PU.1-GATA1 gene circuit of hematopoietic stem cells. Thus, we consider the state $(+, +)$ as stem cells (SC), while the states $(+, +, -)$ and $(-, +, +)$ are downstream transit-amplifying cells (TA1 and TA2). Additionally, the states not included in the above steady states are termed transition cells (TC). These arguments define cell types given by equation (4).

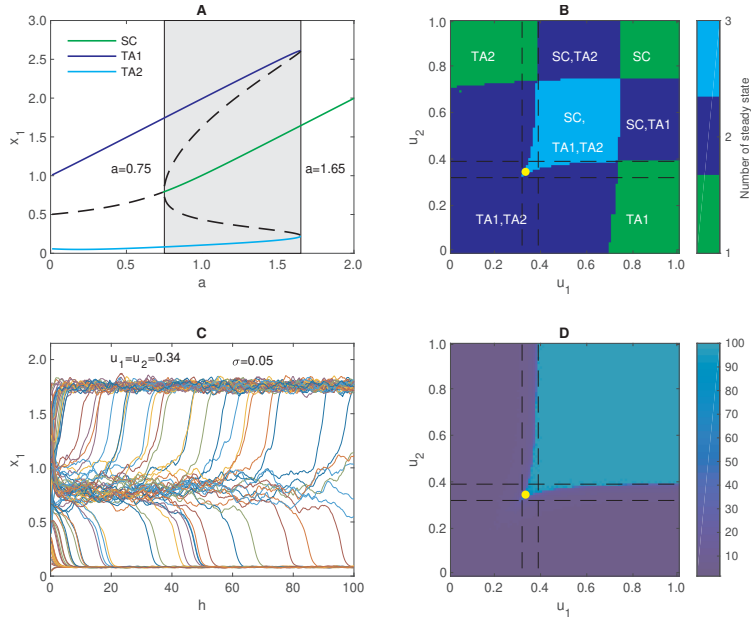


Figure 2: Bifurcation analysis of the gene expression dynamics. (A) Dependence of the steady state solution (in x_1) on the expression rate a ($a_1 = a_2 = a$). Solid lines represent stable steady states, and dashed lines represent unstable steady states. (B) Dependence of the cell types with epigenetic states u_1 and u_2 . The color shows the number of steady states. (C) Sample dynamics of cell state transition obtained by solving the stochastic differentiation equation (1)-(3). Here, $u_1 = u_2 = 0.34$ (the yellow dot in B and in D) and $\sigma = 0.05$. (D) Average duration of the SC state with the epigenetic state (u_1, u_2) .

Considering the effects of epigenetic modifications and extrinsic noise perturbations, the expression rates a_i are expressed as equations (3). To begin

with, we omitted the extrinsic noise by setting $\sigma_1 = \sigma_2 = 0$. The dependence of the phenotypes of steady state on the epigenetic state u_1 and u_2 is shown in Figure 2B. Figure 2B suggests that the three cell types SC, TA1, or TA2 may occur when the epigenetic states of the two genes vary. Specifically, the stem cell state can emerge when $u_1 > 0.4$ and $u_2 > 0.4$.

Next, we set $\sigma = 0.05$ to introduce the noise perturbation. In this case, the gene expression dynamics are described by the random differential equations (1)-(3). To explore the dynamics of cell-type transition under noise perturbations, given the epigenetic state u_1 and u_2 , we set the initial condition following Figure 2B and numerically solve equations (1)-(3) for 100h. Simulations show that TA cells remained unchanged during the simulation. However, for SC with (u_1, u_2) take values near the edge of the SC zone ($u_1 = u_2 = 0.34$), the cell switched to TA cell following random perturbations (Fig. 2C). Figure 2D shows the average duration of the SC state with different epigenetic states (u_1, u_2) . These results indicate that the definition of cell types of SC, TA1, and TA2 is appropriate following the gene regulation dynamics (1)-(3), and the epigenetic state (u_1, u_2) is important for the phenotype of cells.

To further explore the dynamics of cell differentiation induced by noise perturbations in the absence of epigenetic state changes, we investigated the dynamics with the coexistence of SC and TA cells by fixing four sets of epigenetic states: $(u_1, u_2) = (0.5, 0.5), (0.5, 0.6), (0.6, 0.5),$ and $(0.6, 0.6)$. We varied the noise perturbation strength σ ranging from 0 to 1 and ran the model 100 times for each combination of epigenetic states and noise perturbation strength, with an initial population of 100 stem cells and a simulation duration of 1000h.

Figure 3 shows the average ratios of SC and TA cells with different noise perturbation strengths and epigenetic states at the end of the simulation in 100 model runs. The results demonstrate that TA cells emerge only when the extrinsic noise strength is larger than a certain threshold. When $(u_1, u_2) = (0.5, 0.5), (0.5, 0.6)$ or $(0.6, 0.5)$, the TA cells appear only when $\sigma > 0.15$, and when $(u_1, u_2) = (0.6, 0.6)$, TA cells appear only when $\sigma > 0.25$. These imply that strong extrinsic noise is required to drive SC differentiation in the absence of epigenetic state changes. Moreover, Figure 3B and C show that the final fractions of cell types are highly sensitive to the epigenetic state (u_1, u_2) and the extrinsic noise strength σ . The interplay between these two factors plays a crucial role in determining the cell fate and type in the multicellular system.

3.2. Population dynamics of stem cell regeneration and differentiation

To investigate the population dynamics of stem cell regeneration and differentiation, we considered the full model introduced in Section 2. Initially, we ran the model simulation with 100 cells, where the epigenetic state \mathbf{u} and gene expression state \mathbf{x} of each cell were randomly distributed over the ranges $0 < u_i < 1$ and $0 < x_i < 3$, respectively. To examine the population dynamics with different expression rates of the two genes, we tested four sets of parameters: $(\alpha_1, \alpha_2) = (0.4, 0.4), (0.4, 1.0), (1.0, 0.4),$ and $(1.0, 1.0)$. For each set of parameters, we ran the model 30 times up to 2000h to reach the stationary equilibrium. In each case, the cells underwent proliferation, differ-

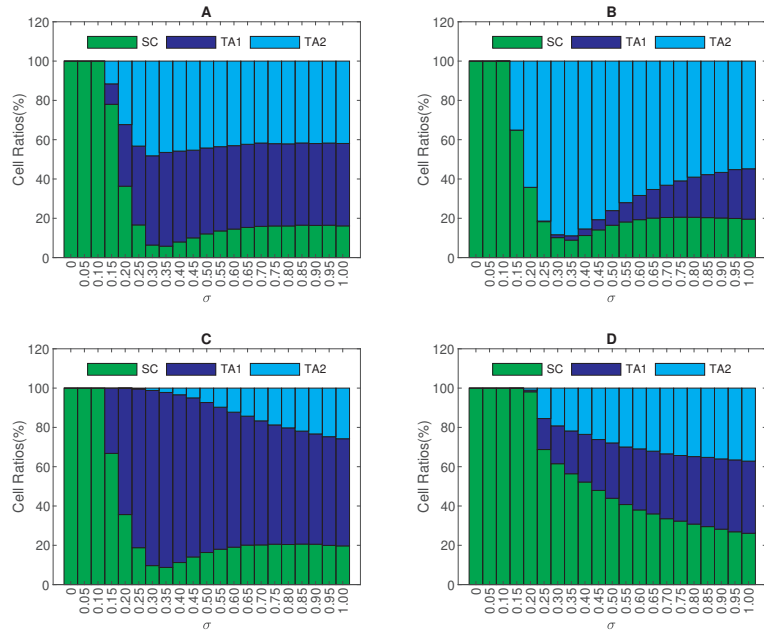


Figure 3: The dynamics of cell differentiation induced by noise perturbations in the absence of epigenetic state changes. Figures show the average ratios of SC and TA cells at the end of 100 model runs with different noise perturbation strengths for different sets of epigenetic states: (A) $(u_1, u_2) = (0.5, 0.5)$, (B) $(u_1, u_2) = (0.5, 0.6)$, (C) $(u_1, u_2) = (0.6, 0.5)$, (D) $(u_1, u_2) = (0.6, 0.6)$. Other parameters remained the same as in Table 2. The statistics are obtained from 100 model runs.

entiation, and cell death, eventually reaching a homeostatic state. Figure 4 shows the four types of population dynamics for different parameter sets. When $(\alpha_1, \alpha_2) = (0.4, 0.4)$, both SC and TA1 and TA2 cells coexisted, indicating the process of self-renewal of stem cells and differentiation to TA1 and TA2 cells (Fig. 4A). When $(\alpha_1, \alpha_2) = (0.4, 1.0)$, only SC and TA2 cells were presented at homeostasis, indicating the blockage of differentiation from stem cells to TA1 cells (Fig. 4B). Similarly, when $(\alpha_1, \alpha_2) = (1.0, 0.4)$, TA2 cells were absent at homeostasis (Fig. 4C), suggesting the blockage of the differentiation from stem cells to TA2 cells. When $(\alpha_1, \alpha_2) = (1.0, 1.0)$, only stem cells were presented at homeostasis, and no stem cell differentiation events occur during the simulation (Fig. 4D). These results indicate that the kinetic parameters of the underlying gene regulation dynamics are crucial for cell phenotypes in homeostasis. In this study, we were interested in the coexistence with SC, TA1, and TA2 cells; thus, we used $(\alpha_1, \alpha_2) = (0.4, 0.4)$ in the following discussions.

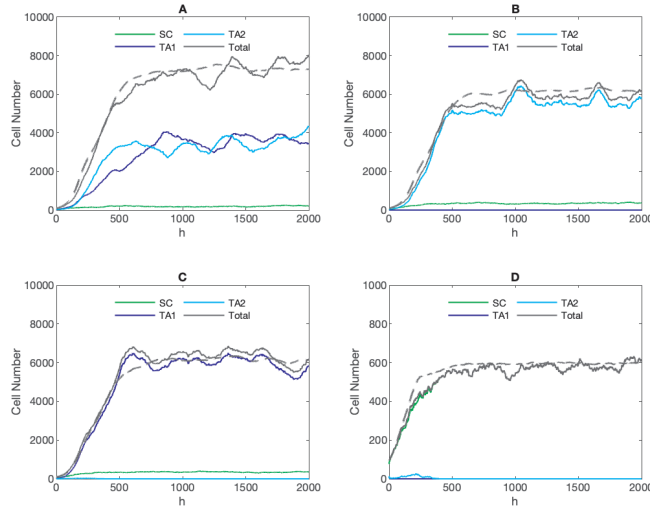


Figure 4: Population dynamics of stem cell regeneration and differentiation. Figures show the evolution dynamics of SC and TA cells number with different parameter sets: (A) $(\alpha_1, \alpha_2) = (0.4, 0.4)$, (B) $(\alpha_1, \alpha_2) = (0.4, 1.0)$, (C) $(\alpha_1, \alpha_2) = (1.0, 0.4)$, (D) $(\alpha_1, \alpha_2) = (1.0, 1.0)$. Other parameters remained the same as in Table 2. The dashed lines represent the averages of the total cell numbers of 30 model runs.

Next, we further investigated the molecular-level dynamics of individual cells. Figure 5A shows the scatter plots of $\mathbf{x} = (x_1, x_2)$ of all cells at different time points ($t = 5, 50, 100, 1000h$). The initially randomly distributed cell states rapidly developed into three clusters corresponding to SC, TA1, and TA2 cells. Accordingly, the epigenetic state $\mathbf{u} = (u_1, u_2)$ of cells rapidly converged to a steady distribution at homeostasis (Fig. 5B). Interestingly, despite the continuous distribution of (u_1, u_2) , the expression states (x_1, x_2) shown discrete

cell types at homeostasis. The bifurcation analysis in Figure 2 suggests that continuous changes in the epigenetic state \mathbf{u} can lead to transitions of cell types defined by the gene expression state \mathbf{x} . These results indicated that continuous changes in the epigenetic state during stem cell regeneration can lead to discontinuous cell fate decisions, providing a mechanism of stem cell differentiation driven by random inheritance of epigenetic state during cell division.

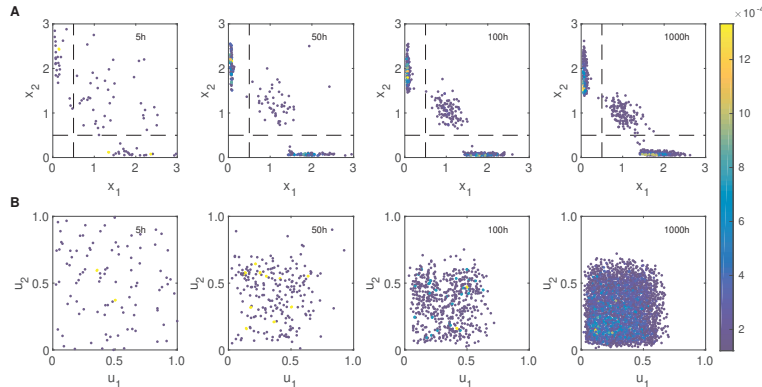


Figure 5: The evolution of gene and epigenetic modifications for the population dynamics shown in Figure 4A. (A) Scatter plots of (x_1, x_2) at different time points ($t = 1, 50, 100, 1000\text{h}$). (B) Scatter plots of (u_1, u_2) at different points ($t = 5, 50, 100, 1000\text{h}$). Parameters are the same as in Table 2.

3.3. Dynamics of transdifferentiation and dedifferentiation

The above simulations demonstrated the differentiation dynamics from stem cells to TA cells, a process commonly occurring during development and tissue homeostasis. However, in various biological processes, transdifferentiation and dedifferentiation are also observed, wherein differentiated cells may lose their phenotype and convert to another cell type or revert to an undifferentiated state[11, 53, 54, 55]. In this context, we have observed that the random inheritance of epigenetic states can induce the differentiation of stem cells. We now explore whether this mechanism can also lead to transdifferentiation and dedifferentiation. To investigate this, we recorded the cell type changes over a long simulation and counted the number of events of cell type changes in each cell division. The average results of 30 model runs are summarized as the transition probability in each cell division in Table 3.

Table 3: Cell state transition probabilities (%) from mother to daughter cells at one cell division. The probability values were calculated from the average over 30 model runs.

	SC	TA1	TA2
SC	73.9402	12.9889	13.0709
TA1	0.0013	99.9955	0.0032
TA2	0.0013	0.0035	99.9952

From the results in Table 3, stem cells predominantly underwent self-renewal with a probability of 73.9402%, or transit to either TA1 or TA2 cells with probabilities of 12.9889% or 13.0709%, respectively, during each cell cycle. However, the TA cells are highly inclined self-renewal, with probabilities exceeding 99.99%. Nevertheless, rare events of transdifferentiation (from TA1 to TA2 or from TA2 to TA1) and dedifferentiation (from TA1 or TA2 to SC) did occur in our simulations, albeit with extremely low frequencies. It is important to note that the transition probabilities depend on the model parameters. In the next section, we discuss how changes in model parameters may affect the frequencies of transdifferentiation and dedifferentiation. Figure 6 shows the transition trajectories of dedifferentiation and transdifferentiation from model simulations in the phase plane of gene expressions. Figure 6C-D shows that the TA states can switch to each other without an intermediate SC state, which suggests evidence of transdifferentiation.

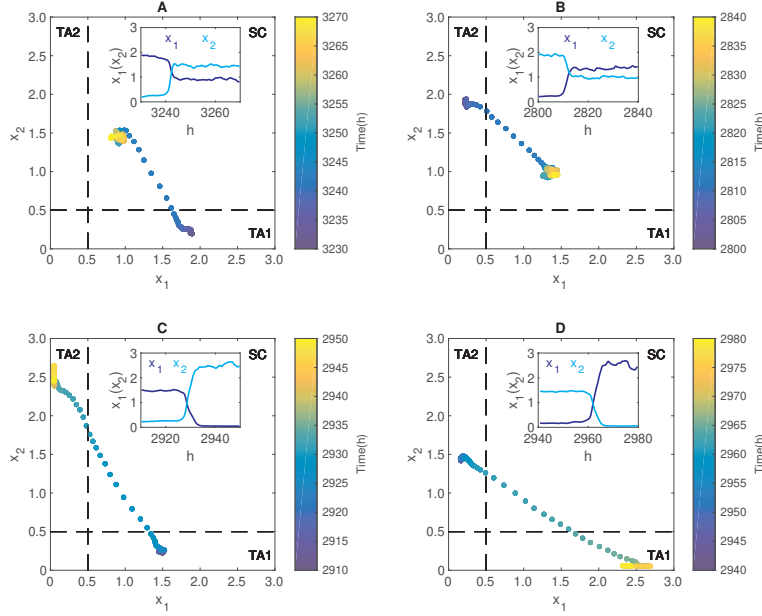


Figure 6: Transition trajectories of dedifferentiation, and transdifferentiation in the phase plane. (A) The dedifferentiation trajectory TA1-SC. (B) The dedifferentiation trajectory TA2-SC. (C) The transdifferentiation trajectory TA1-TA2. (D) The transdifferentiation trajectory TA2-TA1. Color bars show the timing in the simulation. Insets show the corresponding temporal dynamics $x_1(t)$ and $x_2(t)$. Parameters were the same as in Table 2.

3.4. The effects of extrinsic noise and epigenetic state inheritance on homeostasis and cell-type transitions

In this section, we explore the impact of extrinsic noise and epigenetic state inheritance on the system's homeostasis and the probabilities of cell-type transitions. From Figure 3, cell-type transitions would not happen when the extrinsic

noise is weak and in the absence of epigenetic state changes. Moreover, when the noise strength σ increases to $\sigma = 0.2$, stem cells may become extinct due to the large differentiation rate (data not shown). Here, we considered the combination of extrinsic noise and epigenetic state changes and assumed a weak extrinsic noise ($\sigma \leq 0.1$).

3.4.1. Effect of extrinsic noise

We began by varying the noise perturbation strength σ from 0 to 0.1 and analyzing the homeostasis cell numbers and transition probabilities. For each value of σ , we conducted model simulation for a time scope of 4000h so that there are enough data for statistics, and considered the results from 2000h to 4000h for further analysis. Similar to the previous simulations, the cells developed into SC or TA cells and approached homeostasis. The numbers of different cell types at homeostasis was insensitive to changes in the noise strength (Fig. 7A). The ratios of different types were largely unaffected by the noise strength (Fig. 7B). These findings indicate that changes in extrinsic noise have minimal impact on the system's state at homeostasis.

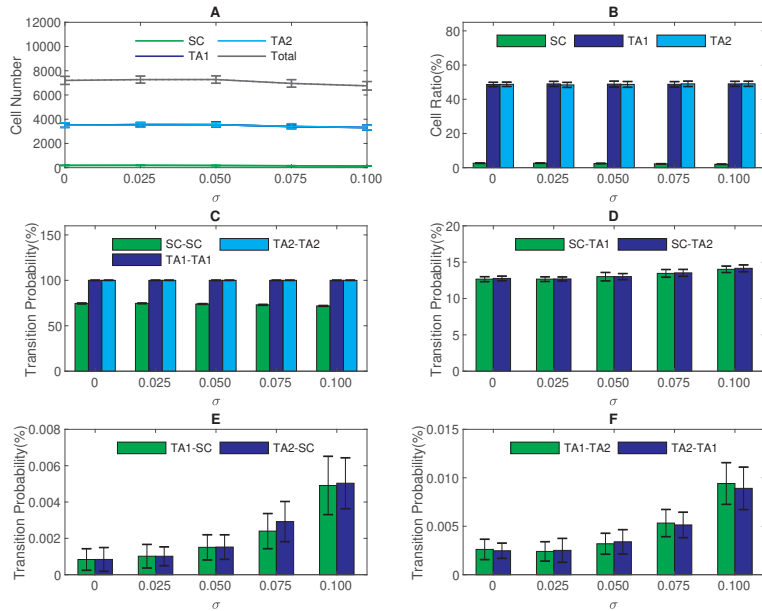


Figure 7: The impact of extrinsic noise on homeostasis and cell state transition. (A) Numbers of different cell types at homeostasis. (B) Ratios of SC and TA cells at homeostasis. (C) The probability of self-renewal in each cell division for different cell types. (D) The probability of differentiation (SC-TA1, SC-TA2) in each cell division. (E) The probability of dedifferentiation (TA1-SC, TA2-SC) in each cell division. (F) The probabilities of transdifferentiation (TA1-TA2, TA2-TA1) in each cell division. All values are calculated from the time scope of 2000h to 4000h in the model simulation. Other parameters were the same as in Table 2. The statistics are obtained from 30 model runs.

Next, we investigated the transition probabilities between different cell types under varying noise strengths (Figure 7C-F). The probabilities of self-renewal (SC-SC, TA1-TA1, TA2-TA2) was found to be unaffected by changes in the noise strength (Fig. 7C). The probabilities of differentiation (SC-TA1 and SC-TA2) showed increases with the noise strength σ (Fig. 7D); accordingly, the probabilities of dedifferentiation (TA1-SC and TA2-SC) increases with σ (Fig. 7E). Likewise, the probabilities of transdifferentiation (TA1-TA2 and TA2-TA1) showed slight increases with σ (Fig. 7F). These results suggest that alterations in the extrinsic noise perturbation have minor effects on cell-type transition rates. Therefore, weak extrinsic noise might not be the primary driving force behind cell-type transitions.

3.4.2. Effect of epigenetic state inheritance

Next, we investigated how random changes in epigenetic modifications may affect the system’s homeostasis and cell-type transitions. To this end, we considered the functions $\phi_i(\mathbf{v})$ in (7), which define the inheritance function of epigenetic states. We varied the parameter m_2 over the interval $[0.8, 0.9]$ and investigated how the cell numbers and transition probabilities may change with m_2 . Here, we fixed $\sigma = 0.05$, while other parameters remained the same as in Table 2. The simulations revealed that as m_2 increased, the numbers of TA cells decreased, while the SC number increased, leading to a decrease in the total cell number (Fig. 8A). Consequently, the ratio of SC increased while the ratio of TA1 and TA2 decreased (Fig. 8B). These results demonstrate that alterations in the inheritance functions of epigenetic states significantly impact the system’s homeostasis.

Further examining the probabilities of cell differentiation, transdifferentiation, and dedifferentiation, we found that the probabilities of self-renewal for TA cells were mostly unaffected by changes in m_2 , while the self-renewal probability of SC increased m_2 (Fig. 8C). Consequently, the differentiation probabilities (SC-TA1 and SC-TA2) markedly decreased with increasing m_2 (Fig. 8D), and the dedifferentiation probabilities (TA1-SC and TA2-SC) increased with m_2 (Fig. 8E). The transdifferentiation probabilities (TA1-TA2 and TA2-TA1) showed an initial increase followed by a decrease as m_2 was raised. Biologically, the function $\phi_i(\mathbf{v})$ represents the expectation of the epigenetic state of daughter cells given the state \mathbf{v} of the mother cells, and m_2 can be used to quantify the activities of enzymes that regulate epigenetic modification. Increasing the parameter m_2 upregulates the epigenetic states u_i of daughter cells. These results suggest that manipulating epigenetic modifications can be a viable strategy to induce transdifferentiation and dedifferentiation.

The aforementioned results were achieved assuming symmetric parameters. In order to explore the impact of asymmetric parameters, we manipulated the gene X_1 parameters and conducted model simulations. The transition probabilities in each cell division under distinct parameters are shown in Figure 9. The results reveal that asymmetric parameters do not significantly deviate from the principal findings obtained using the assumption of symmetrical parameters. It is worth noting that increases in k_1 and s_1 correspond to an increase in the

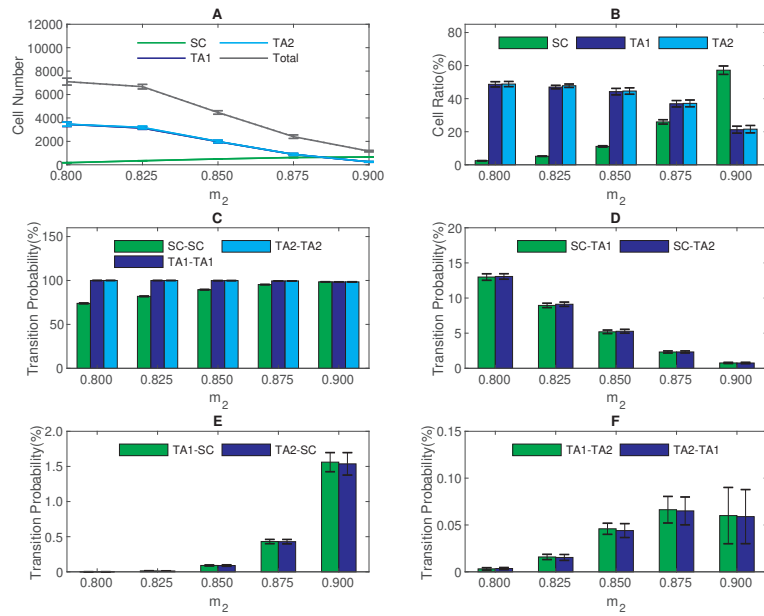


Figure 8: The impact of epigenetic state inheritance function on homeostasis and cell state transition. (A) Numbers of different cell types at homeostasis. (B) Ratios of SC and TA cells at homeostasis. (C) The probability of self-renewal in each cell division of different cell types. (D) The probability of differentiation (SC-TA1, SC-TA2) in each cell division. (E) The probability of dedifferentiation (TA1-SC, TA2-SC) in each cell division. (F) The probabilities of transdifferentiation (TA1-TA2, TA2-TA1) in each cell division. All values are calculated from the time scope of 2000h to 4000h in the model simulation. Other parameters were the same as in Table 2. The statistics are obtained from 30 model runs.

differentiation rate SC-TA2 (Fig. 9B) and a decrease in the dedifferentiation rate TA2-SC (Fig. 9D). Conversely, increases in α_1 and ρ_1 values lead to a reduction in the differentiation rate SC-TA2 (Fig. 9B) and an increase in the dedifferentiation rate TA2-SC (Fig. 9D).

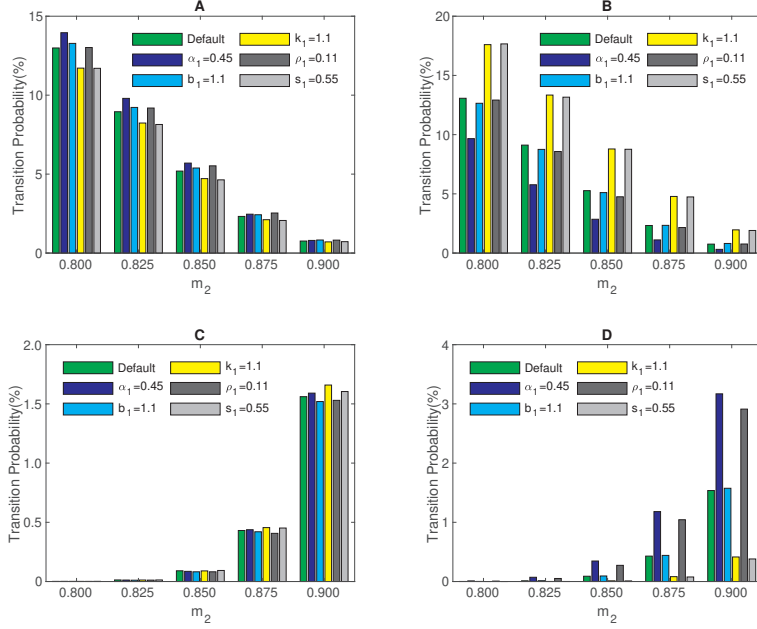


Figure 9: Transition probability with asymmetry parameters. (A) The transition probability of differentiation SC-TA1 in each cell division. (B) The transition probability of SC-TA2 in each cell division. (C) The probability of dedifferentiation rate TA1-SC in each cell division. (D) The probability of dedifferentiation rate TA2-SC in each cell division. Other parameters were the same as in Table 2. The statistics were obtained from 30 model runs.

3.5. Dynamics of cell reprogramming through the induction of transcription factors

The previous simulations explored the mechanisms of cell transdifferentiation and dedifferentiation induced by extrinsic noise and epigenetic modifications. In this section, we investigate the dynamics of cell reprogramming through the induction of transcription factors.

We considered introducing an external transcription factor that enhances the transcription of the self-activation of the X_1 gene. Consequently, the equations governing the gene regulation network dynamics are modified as follows:

$$\begin{cases} \frac{dx_1}{dt} = (a_1 + a_{TF}) \left(\rho_1 + (1 - \rho_1) \frac{x_1^n}{s_1^n + x_1^n} \right) + b_1 \frac{s_2^n}{s_2^n + x_2^n} - k_1 x_1, \\ \frac{dx_2}{dt} = a_2 \left(\rho_2 + (1 - \rho_2) \frac{x_2^n}{s_2^n + x_2^n} \right) + b_2 \frac{s_1^n}{s_1^n + x_1^n} - k_2 x_2. \end{cases} \quad (8)$$

Here, a_{TF} represents the augmentation factor for the activation rate caused by the introduced transcription factor.

To simulate the dynamics of cell reprogramming, we fixed $\sigma = 0.05$, $m_2 = 0.8$, and varied a_{TF} from 0 to 0.5, keeping other parameters the same as in Table 2. In model simulations, the first event is presumably a transition from TA cells to stem cells, and then the system evolves towards the steady state distribution of cell types. We defined successful stem cell induction as the occurrence of 100 stem cells. First, we initialized the system with 500 differentiated cells (either 100% TA1 cells or 100% TA2 cells) and conducted model simulations for 10000h to examine the potential to induce stem cells. When the system initiated with TA1 cells, the probability of successful induction at the end of simulations showed a slight increase and then remained relatively low and stable with varying a_{TF} (Fig. 10A). Conversely, when initiated with TA2 cells, the probability of successful induction at the end of simulations increased with a_{TF} , and reached a probability of near 100% when a_{TF} is large enough (Fig. 10A). Since the factor a_{TF} only affects the transcription of X_1 , the introduction of stem cells from TA1 cells is mainly due to the basal dedifferentiation shown in Table 3. Thus, the extra induction probability from TA2 cells comes from the effect of a_{TF} . Moreover, we calculate the timing of successful induction in each situation. For the system initiated with TA1 cells, the time required for successful stem cell induction is about 600h with varying a_{TF} (Fig. 10B). However, when initiated with TA2 cells, the time of stem cell induction showed an obvious decrease with the increasing of a_{TF} , with the time of 400h when $a_{TF} > 0.4$ (Fig. 10B). We further show the population dynamics after the induction of a_{TF} (Figure 10C). The dynamics reveal that for cells initialized with 100% TA2 cells, stem cells begin to appear after approximately 300h due to the dedifferentiation of TA2 cells. Subsequently, stem cells differentiate into TA1 and TA2 cells, insulating a cell population approaching homeostasis with all three cell types.

Furthermore, we examined the homeostasis cell numbers and the transition probabilities. We initialized 100 stem cells for statistical simplicity and varied a_{TF} from 0 to 0.2. We then conducted model simulations for a time scope of 4000h and analyzed the results from 2000h to 4000h. Consequently, the number of TA1 cells increased with higher values of a_{TF} , while the number of TA2 cells decreased (Fig. 11A). The ratios of TA1 cells and stem cells increased with a_{TF} , whereas the ratio of TA2 cells decreased with increasing a_{TF} (Fig. 11B). Subsequently, we analyzed the transition probabilities for different values of a_{TF} . The self-renewal probability at each cell division remained unaffected by variations in a_{TF} , while changes in a_{TF} significantly influenced the probabilities of differentiation, transdifferentiation, and dedifferentiation. Specifically, increasing a_{TF} reduced the differentiation from SC to TA2 cells, promote the dedifferentiation from TA2 cells to SC, and alter the transdifferentiation between TA1 and TA2 cells, resulting in an increase in the TA2-TA1 transition probability and a decrease in the TA1-TA2 transition probability (Fig. 11C-F).

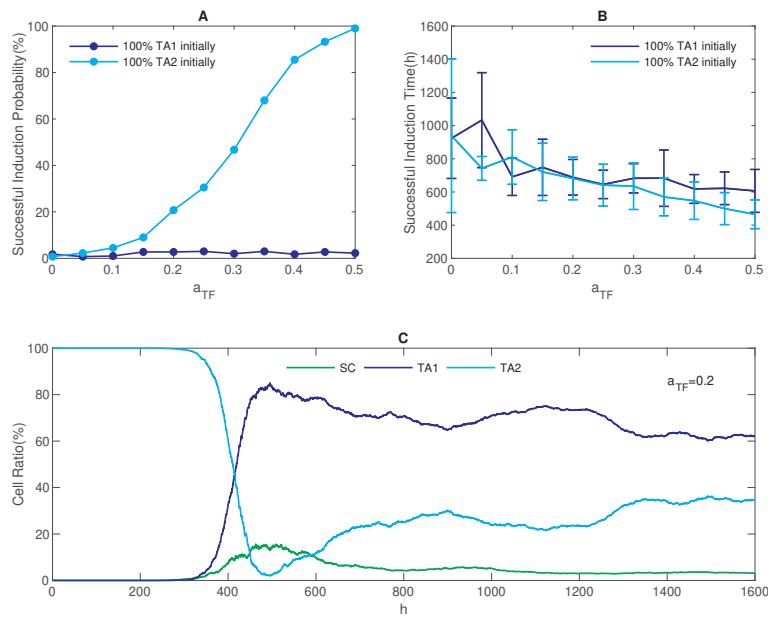


Figure 10: Dynamics of cell reprogramming through the induction of transcription factors. (A) The probability of successful stem cell induction. (B) The time required for successful stem cell induction. (C) Time evolution of cell ratios starting from 100% TA2 cells. Other parameters were the same as in Table 2. The statistics were obtained from 600 model runs.

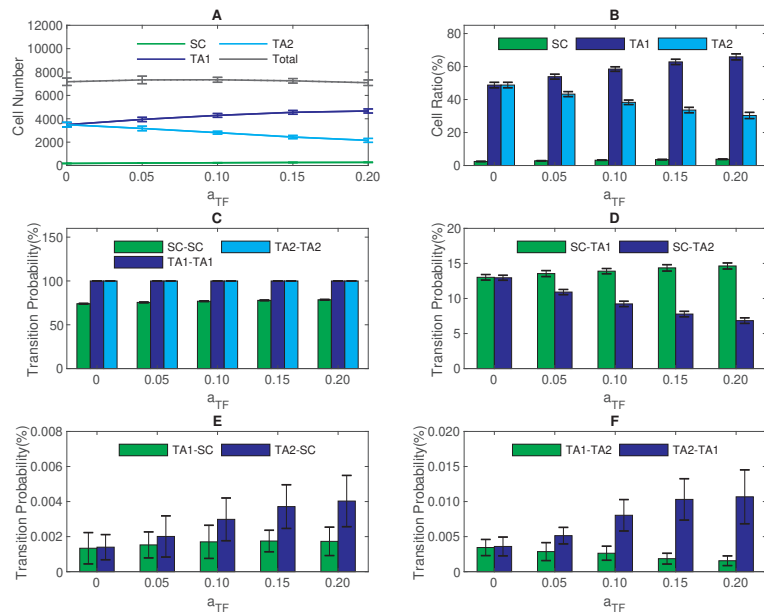


Figure 11: The effect of transcription factor introduction on cell number and cell state transition. (A) Numbers of different types of cells at homeostasis. (B) The cell ratios for different cell types over the period from 2000h to 4000h. (C)-(F) The cell transition probabilities. Other parameters were the same as in Table 2. The statistics were obtained from 30 model runs.

3.6. Waddington landscape

To gain further insights into the influence of extrinsic noise and epigenetic state inheritance on cell fate decisions during tissue growth, we delve into the temporal evolution of Waddington landscape based on our simulation results. The numerical scheme described above yields the cell count $N(t, \mathbf{x})$ at time t with state $\mathbf{x} = (x_1, x_2)$. The total cell number is given by $N(t) = \int N(t, \mathbf{x}) d\mathbf{x}$. Consequently, we defined $f(t, \mathbf{x}) = N(t, \mathbf{x})/N(t)$ as the frequency of cells with state \mathbf{x} . This enables us to define the evolution of Waddington’s epigenetic landscape as follows:

$$U(t, \mathbf{x}) = -\log(1 + f(t, \mathbf{x})), \quad (9)$$

where the introduction of the number 1 prevents issues arising from zero frequency.

Figure 12 illustrates landscapes that vary with extrinsic noise strength (σ), epigenetic regulation parameter (m_2), and the introduction of an extra factor (a_{TF}) in cell reprogramming. As demonstrated in Figure 12A, the landscape remains largely unaffected by changes in the extrinsic noise strength. This observation aligns with the above discussion, which revealed that alterations in the extrinsic noise do not impact the homeostatic state of the system (Fig. 7). However, the landscapes exhibit notable changes as the parameter m_2 increases from 0.8 to 0.9 (Fig. 12B). Elevated values of m_2 lead to a higher proportion of stem cells in the stationary state, indicating the induction of dedifferentiation through alterations in epigenetic regulation. Moreover, the introduction of the extra factor a_{TF} in (8) disrupts the balance between TA1 and TA2 cells, resulting in a greater fraction of TA1 cells (Fig. 12C). These findings underscore the substantial role of varying epigenetic regulation and introducing an extra transcription factor in reshaping the Waddington landscape.

4. Discussion

The intricate regulation of stem cell differentiation and tissue development is a cornerstone challenge in the realms of developmental biology and regenerative medicine. Over time, various mechanisms have been postulated to induce crucial biological processes like cell differentiation, dedifferentiation, and transdifferentiation[56, 57, 58, 59]. These mechanisms include stochastic fluctuations, modification to gene regulation networks, the induction of external transcription factors, and the manipulation of small molecules. Yet, while these mechanisms offer valuable insights, they fall short of capturing the inherent progression of cell lineage and the complexity of cellular heterogeneity.

Recent research challenges the prevailing model that assumes changing gene expression within a bistable region is sufficient to alter cell fate[60]. The study by Hoppe et al. demonstrated that random fluctuations of PU.1 and GATA1 expression are insufficient to initiate the cell-fate decision between megakaryocyte/erythroid (MegE) and granulocyte/monocyte (GM) lineages. Long-term absolute protein levels in single differentiating HSCs and their progeny were

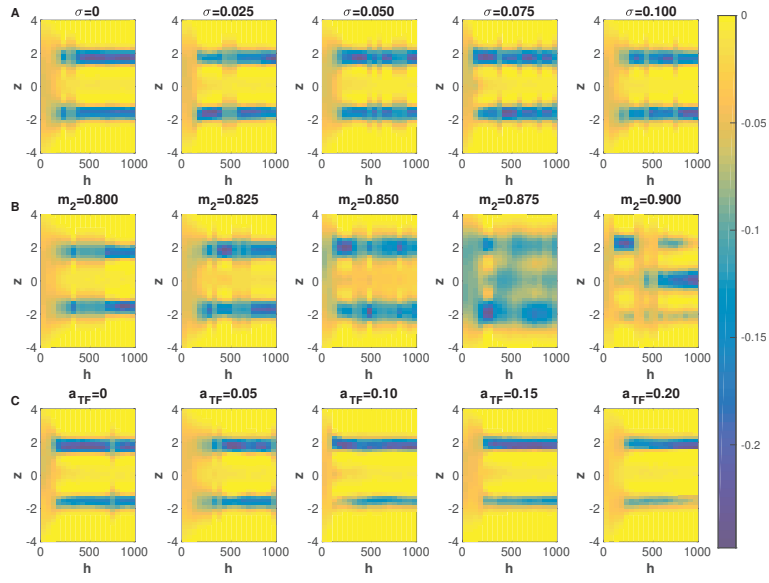


Figure 12: Waddington landscape. (A) Temporal evolution of the Waddington landscape with varying extrinsic noises. (B) Temporal evolution of the Waddington landscape with varying epigenetic regulation parameter m_2 . (C) Temporal evolution of the Waddington landscape with varying extra factor a_{TF} in cell reprogramming. The Waddington landscapes are visualized as heatmaps for the function $U(t, z)$ with $z = x_1 - x_2$. Other parameters were the same as in Table 2.

quantified, which showed that multiple generations are required to induce changes in PU.1 and GATA1 protein levels, and these transcription factors are only executing and reinforcing lineage choice once made[60]. These observations pointed to the significant roles of cell division in guiding cell fate decisions. Additionally, the profound impact of epigenetic regulation on cellular heterogeneity and phenotype transitions has garnered considerable attention[27, 61, 62, 63, 64, 65].

In our pursuit to quantitatively dissect the dynamics of cell-type transitions driven by epigenetic modifications, we developed a comprehensive hybrid model for stem cell regeneration. This model integrates gene regulation networks, epigenetic state inheritance, and cell regeneration dynamics. The essence of our model lies in its ability to simulate the biological process of cell population growth and the establishment of homeostasis, characterized by a delicate equilibrium among diverse cell types. Our simulations unravel a mechanism where stochastic inheritance of epigenetic modifications leads to spontaneous switches in cellular phenotypes during cell cycling. We argue that the natural biological process of the cell cycle and stochastic inheritance during cell division can serve as the driving force of cell-type transition. The interplay between random epigenetic transition and the intrinsic dynamics of gene networks emerges as a linchpin in steering cell-type switches and consolidating cellular stability. Remarkably, our findings underscore how manipulations in epigenetic regulation can wield influence over the epigenetic landscape, thereby augmenting the potential for cell dedifferentiation and transdifferentiation.

The Waddington landscape serves as a core concept in understanding the mechanisms of stem cell differentiation and cellular plasticity[66, 67]. Traditionally, the stochastic dynamics of gene regulatory networks find gene expressions through Langevin equations, or their associated formulations like the master equation or Fokker-Planck equation. At the heart of this landscape lies the Waddington potential, $U = -\ln(P_{ss})$, intricately linked to the stationary distribution P_{ss} of the master equation or Fokker-Planck equation[37, 68, 69]. This potential is pivotal in revealing the phenotypic outcomes tethered to the underlying regulatory network. However, it falls short of encapsulating the dynamic processes of cell-type transitions during development and tissue growth without considering the cell cycle process.

In this context, our study charts a pioneering path by introducing a computational model framework that fuses the mechanics of cell regeneration with the ebbs and flows of epigenetic modifications during cell division. This model allows us to quantitatively map the relationship between alterations in the epigenetic landscape and corresponding phenotypic transitions. Our model simulations breathe life into the concept of temporal potential in a biological context, providing an innovative lens to explore the evolving dynamics of the Waddington landscape throughout tissue growth. With this endeavor, we not only unravel novel insights into the intricate mechanisms governing stem cell differentiation and cell reprogramming but also offers a promising path to enhance the field of regenerative medicine[53, 70].

In conclusion, our research sets forth a novel paradigm by integrating the interplay of gene networks, epigenetic state inheritance, and cell regeneration

dynamics. Through detailed computational simulations and biological insights, we shed light on the underlying forces steering cell fate decisions. The holistic understanding gained from our model has the potential to catalyze transformative breakthroughs in regenerative medicine, propelling us closer to unlocking the full regenerative potential of cells and tissues.

Acknowledgements

This work is supported by the National Natural Science Foundation of China (No.11831015) and the Science and Technology Project (No.JAT200246) funded by the Education Department of Fujian Province, China.

References

References

- [1] H. Clevers, What is an adult stem cell?, *Science* 350 (6266) (2015) 1319–1320. doi:10.1126/science.aad7016.
- [2] C. H. Waddington, The epigenotype, *Int J Epidemiol* 41 (1) (2012) 10–13. doi:10.1093/ije/dyr184.
- [3] J. E. Ferrell, Bistability, bifurcations, and Waddington’s epigenetic landscape, *Curr Biol* 22 (11) (2012) R458–R466. doi:10.1016/j.cub.2012.03.045.
- [4] M. K. Jolly, D. Jia, M. Boareto, S. A. Mani, K. J. Pienta, E. Ben-Jacob, H. Levine, Coupling the modules of EMT and stemness: a tunable ‘stemness window’ model, *Oncotarget* 6 (28) (2015) 25161–25174. doi:10.18632/oncotarget.4629.
- [5] J. Wang, K. Zhang, L. Xu, E. Wang, Quantifying the Waddington landscape and biological paths for development and differentiation, *Proc Natl Acad Sci USA* 108 (20) (2011) 8257–8262. doi:10.1073/pnas.1017017108.
- [6] N. Iovino, G. Cavalli, Rolling ES cells down the Waddington landscape with Oct4 and Sox2, *Cell* 145 (6) (2011) 815–817. doi:10.1016/j.cell.2011.05.027.
- [7] J. X. Zhou, S. Huang, Understanding gene circuits at cell-fate branch points for rational cell reprogramming, *Trends Genet* 27 (2) (2011) 55–62. doi:10.1016/j.tig.2010.11.002.
- [8] M. K. Rommelfanger, A. L. MacLean, A single-cell resolved cell-cell communication model explains lineage commitment in hematopoiesis, *Development* 148 (24) (2021) dev199779. doi:10.1242/dev.199779.

- [9] L. Xu, K. Zhang, J. Wang, Exploring the mechanisms of differentiation, dedifferentiation, reprogramming and transdifferentiation, *PLoS One* 9 (8) (2014) e105216. doi:10.1371/journal.pone.0105216.
- [10] R. Losick, C. Desplan, Stochasticity and cell fate, *Science* 320 (5872) (2008) 65–68. doi:10.1126/science.1147888.
- [11] C. Cobaleda, W. Jochum, M. Busslinger, Conversion of mature B cells into T cells by dedifferentiation to uncommitted progenitors, *Nature* 449 (7161) (2007) 473–477. doi:10.1038/nature06159.
- [12] Q. Zhou, D. A. Melton, Extreme makeover: converting one cell into another, *Cell Stem Cell* 3 (4) (2008) 382–388. doi:10.1016/j.stem.2008.09.015.
- [13] Q. Zhou, J. Brown, A. Kanarek, J. Rajagopal, D. A. Melton, In vivo reprogramming of adult pancreatic exocrine cells to β -cells, *Nature* 455 (7213) (2008) 627–632. doi:10.1038/nature07314.
- [14] S. Yamanaka, Induced pluripotent stem cells: past, present, and future, *Cell Stem Cell* 10 (6) (2012) 678–684. doi:10.1016/j.stem.2012.05.005.
- [15] G. Amabile, A. Meissner, Induced pluripotent stem cells: current progress and potential for regenerative medicine, *Trends Mol Med* 15 (2) (2009) 59–68. doi:10.1016/j.molmed.2008.12.003.
- [16] J. Shu, C. Wu, Y. Wu, Z. Li, S. Shao, W. Zhao, X. Tang, H. Yang, L. Shen, X. Zuo, W. Yang, Y. Shi, X. Chi, H. Zhang, G. Gao, Y. Shu, K. Yuan, W. He, C. Tang, Y. Zhao, H. Deng, Induction of pluripotency in mouse somatic cells with lineage specifiers, *Cell* 153 (5) (2013) 963–975. doi:10.1016/j.cell.2013.05.001.
- [17] C. Angermueller, S. J. Clark, H. J. Lee, I. C. Macaulay, M. J. Teng, T. X. Hu, F. Krueger, S. A. Smallwood, C. P. Ponting, T. Voet, G. Kelsey, O. Stegle, W. Reik, Parallel single-cell sequencing links transcriptional and epigenetic heterogeneity, *Nat Methods* 13 (3) (2016) 229–232. doi:10.1038/nmeth.3728.
- [18] A. A. Pollen, T. J. Nowakowski, J. Shuga, X. Wang, A. A. Leyrat, J. H. Lui, N. Li, L. Szpankowski, B. Fowler, P. Chen, N. Ramalingam, G. Sun, M. Thu, M. Norris, R. Lebofsky, D. Toppani, D. W. Kemp, M. Wong, B. Clerkson, B. N. Jones, S. Wu, L. Knutsson, B. Alvarado, J. Wang, L. S. Weaver, A. P. May, R. C. Jones, M. A. Unger, A. R. Kriegstein, J. A. A. West, Low-coverage single-cell mRNA sequencing reveals cellular heterogeneity and activated signaling pathways in developing cerebral cortex, *Nat Biotechnol* 32 (10) (2014) 1053–1058. doi:10.1038/nbt.2967.
- [19] A. P. Patel, I. Tirosh, J. J. Trombetta, A. K. Shalek, S. M. Gillespie, H. Wakimoto, D. P. Cahill, B. V. Nahed, W. T. Curry, R. L. Martuza,

- D. N. Louis, O. Rozenblatt-Rosen, M. L. Suvà, A. Regev, B. E. Bernstein, Single-cell RNA-seq highlights intratumoral heterogeneity in primary glioblastoma, *Science* 344 (6190) (2014) 1396–1401. doi:10.1126/science.1254257.
- [20] S. Huang, Non-genetic heterogeneity of cells in development: more than just noise, *Development* 136 (23) (2009) 3853–3862. doi:10.1242/dev.035139.
- [21] Å. K. Björklund, M. Forkel, S. Picelli, V. Konya, J. Theorell, D. Friberg, R. Sandberg, J. Mjösberg, The heterogeneity of human CD127+ innate lymphoid cells revealed by single-cell RNA sequencing, *Nat Immunol* 17 (4) (2016) 451–460. doi:10.1038/ni.3368.
- [22] M. B. Johnson, P. P. Wang, K. D. Atabay, E. A. Murphy, R. N. Doan, J. L. Hecht, C. A. Walsh, Single-cell analysis reveals transcriptional heterogeneity of neural progenitors in human cortex, *Nat Neurosci* 18 (5) (2015) 637–646. doi:10.1038/nn.3980.
- [23] A. K. Shalek, R. Satija, X. Adiconis, R. S. Gertner, J. T. Gaublumme, R. Raychowdhury, S. Schwartz, N. Yosef, C. Malboeuf, D. Lu, J. J. Trombetta, D. Gennert, A. Gnirke, A. Goren, N. Hacohen, J. Z. Levin, H. Park, A. Regev, Single-cell transcriptomics reveals bimodality in expression and splicing in immune cells, *Nature* 498 (7453) (2013) 236–240. doi:10.1038/nature12172.
- [24] D.-S. Lee, J.-Y. Shin, P. D. Tonge, M. C. Puri, S. Lee, H. Park, W.-C. Lee, S. M. I. Hussein, T. Bleazard, J.-Y. Yun, J. Kim, M. Li, N. Cloonan, D. Wood, J. L. Clancy, R. Mosbergen, J.-H. Yi, K.-S. Yang, H. Kim, H. Rhee, C. A. Wells, T. Preiss, S. M. Grimmond, I. M. Rogers, A. Nagy, J.-S. Seo, An epigenomic roadmap to induced pluripotency reveals DNA methylation as a reprogramming modulator, *Nat Commun* 5 (1) (2014) 5619. doi:10.1038/ncomms6619.
- [25] H. Bagci, A. G. Fisher, DNA demethylation in pluripotency and reprogramming: the role of tet proteins and cell division, *Cell Stem Cell* 13 (3) (2013) 265–269. doi:10.1016/j.stem.2013.08.005.
- [26] B. Zhang, H. Zheng, B. Huang, W. Li, Y. Xiang, X. Peng, J. Ming, X. Wu, Y. Zhang, Q. Xu, W. Liu, X. Kou, Y. Zhao, W. He, C. Li, B. Chen, Y. Li, Q. Wang, J. Ma, Q. Yin, K. Kee, A. Meng, S. Gao, F. Xu, J. Na, W. Xie, Allelic reprogramming of the histone modification H3K4me3 in early mammalian development, *Nature* 537 (7621) (2016) 553–557. doi:10.1038/nature19361.
- [27] A. P. Feinberg, A. Levchenko, Epigenetics as a mediator of plasticity in cancer, *Science* 379 (6632) (2023) eaaw3835. doi:10.1126/science.aaw3835.

- [28] D. Rossetto, N. Avvakumov, J. Côté, Histone phosphorylation: a chromatin modification involved in diverse nuclear events, *Epigenetics* 7 (10) (2012) 1098–1108. doi:10.4161/epi.21975.
- [29] C. Plass, S. M. Pfister, A. M. Lindroth, O. Bogatyrova, R. Claus, P. Lichter, Mutations in regulators of the epigenome and their connections to global chromatin patterns in cancer, *Nat Rev Genet* 14 (11) (2013) 765–780. doi:10.1038/nrg3554.
- [30] A. V. Probst, E. Dunleavy, G. Almouzni, Epigenetic inheritance during the cell cycle, *Nat Rev Mol Cell Biol* 10 (3) (2009) 192–206. doi:10.1038/nrm2640.
- [31] H. Easwaran, H.-C. Tsai, S. B. Baylin, Cancer epigenetics: tumor heterogeneity, plasticity of stem-like states, and drug resistance, *Mol Cell* 54 (5) (2014) 716–727. doi:10.1016/j.molcel.2014.05.015.
- [32] H. Niwa, Y. Toyooka, D. Shimosato, D. Strumpf, K. Takahashi, R. Yagi, J. Rossant, Interaction between Oct3/4 and Cdx2 determines trophoblast differentiation, *Cell* 123 (5) (2005) 917–929. doi:10.1016/j.cell.2005.08.040.
- [33] A. E. Schaffer, K. K. Freude, S. B. Nelson, M. Sander, Nkx6 transcription factors and Ptf1a function as antagonistic lineage determinants in multipotent pancreatic progenitors, *Dev Cell* 18 (6) (2010) 1022–1029. doi:10.1016/j.devcel.2010.05.015.
- [34] A. Ralston, J. Rossant, Genetic regulation of stem cell origins in the mouse embryo, *Clin Genet* 68 (2) (2005) 106–112. doi:10.1111/j.1399-0004.2005.00478.x.
- [35] S. H. Orkin, L. I. Zon, Hematopoiesis: an evolving paradigm for stem cell biology, *Cell* 132 (4) (2008) 631–644. doi:10.1016/j.cell.2008.01.025.
- [36] Y.-H. Loh, J.-H. Ng, H.-H. Ng, Molecular framework underlying pluripotency, *Cell Cycle* 7 (7) (2008) 885–891. doi:10.4161/cc.7.7.5636.
- [37] J. Wang, L. Xu, E. Wang, S. Huang, The potential landscape of genetic circuits imposes the arrow of time in stem cell differentiation, *Biophys J* 99 (1) (2010) 29–39. doi:10.1016/j.bpj.2010.03.058.
- [38] J. Lei, G. He, H. Liu, Q. Nie, A delay model for noise-induced bidirectional switching, *Nonlinearity* 22 (12) (2009) 2845–2859. doi:10.1088/0951-7715/22/12/003.
- [39] D. W. Austin, M. S. Allen, J. M. McCollum, R. D. Dar, J. R. Wilgus, G. S. Sayler, N. F. Samatova, C. D. Cox, M. L. Simpson, Gene network shaping of inherent noise spectra, *Nature* 439 (7076) (2006) 608–611. doi:10.1038/nature04194.

- [40] J. Lei, S. A. Levin, Q. Nie, Mathematical model of adult stem cell regeneration with cross-talk between genetic and epigenetic regulation, *Proc Natl Acad Sci USA* 111 (10) (2014) E880–E887. doi:10.1073/pnas.1324267111.
- [41] J. Lei, A general mathematical framework for understanding the behavior of heterogeneous stem cell regeneration, *J Theor Biol* 492 (2020) 110196. doi:10.1016/j.jtbi.2020.110196.
- [42] J. Lei, Evolutionary dynamics of cancer: from epigenetic regulation to cell population dynamics—mathematical model framework, applications, and open problems, *Sci China Math* 63 (3) (2020) 411–424. doi:10.1007/s11425-019-1629-7.
- [43] A. Moustakas, K. Pardali, A. Gaal, C.-H. Heldin, Mechanisms of TGF- β signaling in regulation of cell growth and differentiation, *Immunol Lett* 82 (1-2) (2002) 85–91. doi:10.1016/S0165-2478(02)00023-8.
- [44] L. Yang, Y. Pang, H. L. Moses, TGF- β and immune cells: an important regulatory axis in the tumor microenvironment and progression, *Trends Immunol* 31 (6) (2010) 220–227. doi:10.1016/j.it.2010.04.002.
- [45] S. Bernard, J. Bélair, M. C. Mackey, Oscillations in cyclical neutropenia: new evidence based on mathematical modeling, *J Theor Biol* 223 (3) (2003) 283–298. doi:10.1016/S0022-5193(03)00090-0.
- [46] A. Doncic, M. Falleur-Fettig, J. M. Skotheim, Distinct interactions select and maintain a specific cell fate, *Mol Cell* 43 (4) (2011) 528–539. doi:10.1016/j.molcel.2011.06.025.
- [47] M. B. Ginzberg, R. Kafri, M. Kirschner, On being the right (cell) size, *Science* 348 (6236) (2015) 1245075. doi:10.1126/science.1245075.
- [48] R. Kafri, J. Levy, M. B. Ginzberg, S. Oh, G. Lahav, M. W. Kirschner, Dynamics extracted from fixed cells reveal feedback linking cell growth to cell cycle, *Nature* 494 (7438) (2013) 480–483. doi:10.1038/nature11897.
- [49] C. Cadart, S. Monnier, J. Grilli, P. J. Sáez, N. Srivastava, R. Attia, E. Terriac, B. Baum, M. Cosentino-Lagomarsino, M. Piel, Size control in mammalian cells involves modulation of both growth rate and cell cycle duration, *Nat Commun* 9 (1) (2018) 3275. doi:10.1038/s41467-018-05393-0.
- [50] E. Zatulovskiy, J. M. Skotheim, On the molecular mechanisms regulating animal cell size homeostasis, *Trends Genet* 36 (5) (2020) 360–372. doi:10.1016/j.tig.2020.01.011.
- [51] R. Huang, J. Lei, Dynamics of gene expression with positive feedback to histone modifications at bivalent domains, *Int J Mod Phys B* 32 (07) (2018) 1850075. doi:10.1142/S0217979218500753.

- [52] R. Huang, J. Lei, Cell-type switches induced by stochastic histone modification inheritance, *Discrete Cont Dyn-B* 24 (10) (2019) 5601–5619. doi:10.3934/dcdsb.2019074.
- [53] C. Jopling, S. Boue, J. C. I. Belmonte, Dedifferentiation, transdifferentiation and reprogramming: three routes to regeneration, *Nat Rev Mol Cell Biol* 12 (2) (2011) 79–89. doi:10.1038/nrm3043.
- [54] S. Collombet, C. van Oevelen, J. L. Sardina Ortega, W. Abou-Jaoudé, B. Di Stefano, M. Thomas-Chollier, T. Graf, D. Thieffry, Logical modeling of lymphoid and myeloid cell specification and transdifferentiation, *Proc Natl Acad Sci USA* 114 (23) (2017) 5792–5799. doi:10.1073/pnas.1610622114.
- [55] S. Thowfeequ, E.-J. Myatt, D. Tosh, Transdifferentiation in developmental biology, disease, and in therapy, *Dev Dyn* 236 (12) (2007) 3208–3217. doi:10.1002/dvdy.21336.
- [56] B. Zhang, P. G. Wolynes, Stem cell differentiation as a many-body problem, *Proc Natl Acad Sci USA* 111 (28) (2014) 10185–10190. doi:10.1073/pnas.1408561111.
- [57] M. Mojtahedi, A. Skupin, J. Zhou, I. G. Castaño, R. Y. Y. Leong-Quong, H. Chang, K. Trachana, A. Giuliani, S. Huang, Cell fate decision as high-dimensional critical state transition, *PLoS Biol* 14 (12) (2016) e2000640. doi:10.1371/journal.pbio.2000640.
- [58] P. S. Stumpf, R. C. Smith, M. Lenz, A. Schuppert, F.-J. Müller, A. Babbie, T. E. Chan, M. P. Stumpf, C. P. Please, S. D. Howison, F. Arai, B. D. MacArthur, Stem cell differentiation as a non-Markov stochastic process, *Cell Syst* 5 (3) (2017) 268–282.e7. doi:10.1016/j.cels.2017.08.009.
- [59] B. Huang, M. Lu, M. Galbraith, H. Levine, J. N. Onuchic, D. Jia, Decoding the mechanisms underlying cell-fate decision-making during stem cell differentiation by random circuit perturbation, *J R Soc Interface* 17 (169) (2020) 20200500. doi:10.1098/rsif.2020.0500.
- [60] P. S. Hoppe, M. Schwarzfischer, D. Loeffler, K. D. Kokkaliaris, O. Hilsenbeck, N. Moritz, M. Endeke, A. Filipczyk, A. Gambardella, N. Ahmed, M. Etzrodt, D. L. Coutu, M. A. Rieger, C. Marr, M. K. Strasser, B. Schaubberger, I. Burtscher, O. Ermakova, A. Bürger, H. Lickert, C. Nerlov, F. J. Theis, T. Schroeder, Early myeloid lineage choice is not initiated by random PU.1 to GATA1 protein ratios, *Nature* 535 (7611) (2016) 299–302. doi:10.1038/nature18320.
- [61] B. Nashun, P. W. Hill, P. Hajkova, Reprogramming of cell fate: epigenetic memory and the erasure of memories past, *EMBO J* 34 (10) (2015) 1296–1308. doi:10.15252/embj.201490649.

- [62] S. S. Ashwin, M. Sasai, Effects of collective histone state dynamics on epigenetic landscape and kinetics of cell reprogramming, *Sci Rep* 5 (1) (2015) 16746. doi:10.1038/srep16746.
- [63] B. Carter, K. Zhao, The epigenetic basis of cellular heterogeneity, *Nat Rev Genet* 22 (4) (2021) 235–250. doi:10.1038/s41576-020-00300-0.
- [64] X. Wang, F. Yu, L. Ye, Epigenetic control of mesenchymal stem cells orchestrates bone regeneration, *Front Endocrinol (Lausanne)* 14 (March) (2023) 1–17. doi:10.3389/fendo.2023.1126787.
- [65] C. Chen, Y. Gao, W. Liu, S. Gao, Epigenetic regulation of cell fate transition: learning from early embryo development and somatic cell reprogramming, *Biol Reprod* 107 (1) (2022) 183–195. doi:10.1093/biolre/i0ac087.
- [66] J. Rajagopal, B. Z. Stanger, Plasticity in the adult: how should the Waddington diagram be applied to regenerating tissues?, *Dev Cell* 36 (2) (2016) 133–137. doi:10.1016/j.devcel.2015.12.021.
- [67] N. Shakiba, C. Li, J. Garcia-Ojalvo, K.-H. Cho, K. Patil, A. Walczak, Y.-Y. Liu, S. Kuehn, Q. Nie, A. Klein, G. Deco, M. Kringelbach, S. Iyer-Biswas, How can Waddington-like landscapes facilitate insights beyond developmental biology?, *Cell Syst* 13 (1) (2022) 4–9. doi:10.1016/j.cels.2021.12.003.
- [68] J. Wang, C. Li, E. Wang, Potential and flux landscapes quantify the stability and robustness of budding yeast cell cycle network, *Proc Natl Acad Sci USA* 107 (18) (2010) 8195–8200. doi:10.1073/pnas.0910331107.
- [69] C. Li, J. Wang, Quantifying Waddington landscapes and paths of non-adiabatic cell fate decisions for differentiation, reprogramming and trans-differentiation, *J R Soc Interface* 10 (89) (2013) 20130787. doi:10.1098/rsif.2013.0787.
- [70] A. Basu, V. K. Tiwari, Epigenetic reprogramming of cell identity: lessons from development for regenerative medicine, *Clin Epigenetics* 13 (1) (2021) 144. doi:10.1186/s13148-021-01131-4.